Gastric Cancer (2022) 25:325–335
https://doi.org/10.1007/s10120-021-01250-0

ORIGINAL ARTICLE

Methylation silencing of *ULK2* via epithelial–mesenchymal transition causes transformation to poorly differentiated gastric cancers

Iori Motoo[1] · Sohachi Nanjo[1] · Takayuki Ando[1] · Satoshi Yamashita[2] · Toshikazu Ushijima[2] · Ichiro Yasuda[1]

Received: 23 June 2021 / Accepted: 9 September 2021 / Published online: 23 September 2021

Abstract

Background Diffuse-type gastric cancers (DGC) typically have a poor prognosis related to their invasion and metastasis, in which the epithelial–mesenchymal transition (EMT) is the initiation step. ULK2 plays a role in the autophagy initiation, which might provide a survival advantage in cancer cells. Although knock-down of *ULK2* reportedly induces autophagy and EMT in a lung cancer cell line, the mechanism of EMT via the down-regulation of *ULK2*, as well as its clinical significance, remains yet unclear. The present study, therefore, aims at clarifying this mechanism and its clinical significance in gastric cancers.

Methods We examined *ULK2* mRNA expression in gastric cancer tissues and normal gastric tissues of healthy people. The effects of knock-downed *ULK2* were examined in two gastric cancer cells, which were investigated in terms of their gene expression changes by the mRNA microarray.

Results ULK2 was strongly expressed in intestinal-type cancers but was scarcely expressed in DGC by immunohistochemical staining. Furthermore, we found that *ULK2* was methylated in DGC and was unmethylated in corresponding adjacent normal tissues. Then, we validated whether knock-down of *ULK2* could induce autophagy, cell migration, and EMT in NUGC3 and MKN45 cells. Using mRNA microarray analysis, we confirmed that knock-down of *ULK2* changed expressions of oncogenic genes associated with cell migration and EMT. Autophagy inhibitor suppressed cell migration and EMT induced by knock-down of *ULK2* in NUGC3 and MKN45.

Conclusion Methylation silencing of *ULK2* could induce cell migration and EMT by means of autophagy induction, causing transformation to poorly differentiated cancers.

Keywords Autophagy · DNA methylation · Cancer development · Epithelial–mesenchymal transition

Introduction

Gastric cancer is one of the most common cancers and the leading cause of cancer-related deaths in the world [1]. The Lauren classification divides gastric cancers into diffuse, intestinal and mixed type [2], with the first (DGC) being histologically characterized as a poorly differentiated adenocarcinoma with poor prognosis [3, 4]. The recent proteomic characterization of gastric cancers showed that DGC can be classified into three groups (PX1-3), of which PX2 and PX3 feature the epithelial–mesenchymal transition (EMT) process [5].

EMT is an essential initiation step in the tumor progression and metastasis, consisting of a process wherein epithelial cells lose cell-to-cell adhesion and apical–basolateral polarization with a fibroblast-like morphology and gain the property to invade the underlying basement membrane [6]. The elucidation of EMT is important for the development of medicines for preventing and treating cancer that shows invasion and metastasis, thereby improving the prognosis.

Autophagy is a mechanism for survival under stress conditions, such as nutrient deprivation, growth factor depletion, drug stimulation, and hypoxia [7]. With regard to tumor development, autophagy might play context-dependent roles in the initiation and the progression of cancer. In the initiation phase, autophagy might act among primary cells as an

Iori Motoo and Sohachi Nanjo share co-first authorship.

✉ Sohachi Nanjo
snanjo@med.u-toyama.ac.jp

[1] Department of Gastroenterology, Graduate School of Medicine and Pharmaceutical Sciences, University of Toyama, 2630 Sugitani, Toyama 930-0194, Japan

[2] Division of Epigenomics, National Cancer Center Research Institute, Tokyo, Japan

anti-carcinogenic mechanism against metabolic stress that causes genetic instability and DNA damage. In the progression phase, autophagy might provide a survival advantage to tumor cells that are under metabolic stress induced by hypoxic and low-nutrient conditions [8]. A previous study showed that some tumor suppressor genes, such as *PTEN*, *PI3K*, *AKT*, and *TP53* inhibit the target of rapamycin signaling pathway upstream [9], and that these might prevent tumor progression through autophagy inhibition. Autophagy impairment is, thus, considered to play an important role in gastric carcinogenesis.

Uncoordinated 51-like kinase 2 (ULK2), a member of the serine/threonine kinase family, plays an essential role in the initiation of autophagy in mammalian cells. Moreover, ULK2 is involved in many other biological processes, including cell fate determination, metabolism, transcriptional control, and oncogenesis [10, 11]. Knock-down of *ULK2* was shown to enhance autophagy and induce EMT in a non-small-cell lung cancer cell line [12]. Methylation silencing of *ULK2* was reported to induce tumor growth in glioblastoma [13]. However, how knock-down of *ULK2* induces EMT and whether *ULK2* is downregulated in gastric cancers with EMT potential has not yet been elucidated. In this regard, we hypothesized that the methylation silencing of *ULK2* in gastric cancer cells can induce EMT in gastric cancers, thereby leading to poorly differentiated cancers.

The present study aims at assessing the mechanism of EMT and its clinical significance in gastric cancers through the down-regulation of *ULK2*. With this, we believe that our findings will help the onward treatment of gastric cancers.

Methods

Clinical tissue samples and Database

Gastric mucosae were obtained by endoscopic biopsy from nine healthy volunteers. Gastric cancer tissues were obtained from 30 gastric cancer patients for reverse transcription (RT)-PCR and quantitative methylation-specific PCR (qMSP), whereas another six gastric cancer patients were retrieved for the methylation microarray analysis. Additionally, formalin-fixed and paraffin embedded (FFPE) tumors were obtained for the immunohistochemical analysis from 14 gastric cancer patients who had undergone surgical resection. For MSP, DNA was extracted from FFPE specimens of ten DGC using the DNeasy Blood & Tissue Kit (Qiagen, Hilden, Germany), according to the manufacturer′s protocol. The Cancer Genome Atlas (TCGA) data and the corresponding clinical files were obtained from the NIH Genomic Data Commons. The methylation levels of *ULK2* were scored using β values, which range from 0 (completely unmethylated) to 1 (completely methylated). Written informed consent was obtained from each subject.

Reagents

Antibodies against microtubule associated protein 1 light chain 3 B (MAP1LC3B) (catalog no. 12741), E-cadherin (catalog no. 3195), and Vimentin (catalog no. 5741) were purchased from Cell Signaling Technology (Danvers, MA). An antibody against p62 (catalog no. P0067) was purchased from Sigma-Aldrich Corporation (St. Louis, MO), an antibody against actin (C-11) (catalog no. sc-1615) was purchased from Santa Cruz Biotechnology (Dallas, TX) and hydroxychloroquine (CQ) (catalog no. S4430) was purchased from Selleckchem (Houston, TX).

Human DNA methylation microarray analysis

As previously described, the genome-wide DNA methylation analysis was performed on clinical samples using the Infinium HumanMethylation450 BeadChip microarray system (Illumina, San Diego, CA). The methylation status of each CpG site was represented by a β value. We used a public database available to analyze the presence of CGI at 200 base pairs upstream from the transcription start site (TSS200) of *Autophagy-related gene* (*Atg*), which was the University of California Santa Cruz Genome Browser (http://genome.ucsc.edu/) on GRCh38/hg38 assembly (Genome Reference Consortium).

Quantitative real-time RT-PCR

RT-PCR was performed using 1 μL of complementary DNA (cDNA), specific primers (Supplementary Table 1), SYBR Green I, and an iCycler Thermal Cycler (Bio-Rad, Richmond, CA). cDNA was synthesized from 1 μg of total RNA using the QuantiTect Reverse Transcription Kit (Qiagen, Hilden, Germany), according to the manufacturer′s protocol. Expression levels of target human genes were normalized to *GAPDH* expression.

MSP, quantitative MSP (qMSP), and de-methylation treatment

Fully methylated DNA and completely unmethylated DNA were prepared by methylating genomic DNA with SssI methylase (New England Biolabs, Beverly, MA) and by amplifying genomic DNA with the GenomiPhi amplification system (GE Healthcare, Little Chalfont, UK), respectively. Bisulfite conversion, MSP, and qMSP were performed with specific primers (Supplementary Table 2), as previously described [14]. Accordingly, the DNA methylation level was

calculated [15] and the de-methylation treatment was performed using stated 1.0 μM 5-aza-2′-deoxycitidine [15].

Immunohistochemistry

Paraffin sections were de-paraffinized and rehydrated, and were incubated with primary antibody against ULK2 (1:500) (ThermoFisher Scientific, Waltham, MA) overnight at 4 °C. Slides were blocked after the antigen retrieval with 5% goat serum for 1 h at room temperature and were then incubated with EnVision + System-HRP labeled polymer anti-rabbit secondary antibody (Dako, Glostrup, Denmark) for 30 min at room temperature. The peroxidase activity was visualized with a diaminobenzidine solution (Dojindo Laboratories, Kumamoto, Japan). The sections were counterstained with hematoxylin, dehydrated, and mounted. The images were acquired with the OLYMPUS BX61 microscope (Olympus, Tokyo, Japan) at 4 × and 10 × magnifications. The expression of ULK2 was estimated on the basis of the percentage and on the intensity of the stained tumor cells. The percentage of the stained positive cells was graded on a numerical scale ranging from 0 to 3, where 0 was 0%, 1 for 0–10%, 2 for 10–50% and 3 for 50–100%. The intensity of the staining was graded on a numerical scale which ranged from 0 to 3, where 0 meant no staining, 1 low-intensity, 2 for moderate and 3 for strong. Respectively, we defined each scale as score 0 for scale 0, score 1 for scale 1, score 5 for scale 2, score 10 for scale 3, with the score index being defined as percentage score × intensity score (range, 0–100). 2 investigators graded and calculated the staining percentage and the staining intensity for the final staining score.

Cell culture

In this study, we used three human gastric cancer cell lines (NUGC3, MKN45, and AGS), where NUGC3 cells were purchased from the Japanese Collection of Research Bioresources (National Institute of Health Sciences, Tokyo, Japan) whereas MKN45 and AGS cells were purchased from the American Type Culture Collection (Rockville, MD). These were maintained in RPMI 1640 (ThermoFisher Scientific) supplemented with 10% fetal bovine serum and 1% Antibiotic–Antimycotic (ThermoFisher Scientific) at 37 °C in a humidified atmosphere with 5% CO_2.

RNA interference

All siRNAs (*siULK2-1* sense: 5′-GCUGGCAGACGUGCUUCAA-AUGAAU-3′ and antisense: 5′-AUUCAUUUGAAGCACGUCUGCCAGC-3′ [HSS114556]; *siULK2-2* sense: 5′-GGAGCAGCUGGUGUUGUACAUGAAA-3′ and antisense: 5′-UUUCA-UGUACAACACCAGCUGCUCC-3′ [HSS114558] were purchased from ThermoFisher Scientific. Cells were transfected using Lipofectamine RNAiMAX (ThermoFisher Scientific) according to the manufacture's protocol. NUGC3 cells were transfected with *siULK2-1* (10 nM) and *siULK2-2* (10 nM) for 48 h. MKN45 cells were transfected with *siULK2-1* (400 nM) and *siULK2-2* (400 nM) for 72 h. Stealth RNAi siRNA Negative Control Hi GC (ThermoFisher Scientific) was used as a negative control.

Migration assay

The transwell migration assay was performed using 24-well Transwell permeable supports with 8-μm pores (Corning Inc., Corning, NY). Mixtures of cells and siRNA were cultured in upper chambers. After 48 or 72 h of incubation, the medium was gently removed and 100 μL of fresh medium containing 10% FBS was added. The lower chamber was filled with 600 μL of medium containing 10% FBS. While using autophagy inhibitors, cells were treated with or without CQ (30 μM). After 24, 48, 72 and 96 h of incubation, membranes were fixed with 4% paraformaldehyde and non-migrated cells on the top side of the membranes were removed with a cotton swab. Membranes were stained with Diff-Quik (JACLaS, Tokyo, Japan), and migrated cells were counted under the OLYMPUS BX61 microscope (Olympus) at a 10 × magnification.

Immunocytochemistry and confocal microscopy

Forty-five thousands cells per well were cultured with siRNA in an 8-well chamber slide (ThermoFisher Scientific). While using autophagy inhibitors, cells were treated with or without CQ (30 μM). After 48 or 72 h, cells were fixed with 4% paraformaldehyde. Slides were incubated with BlockAce (KAC, Kyoto, Japan) at room temperature for 1 h and were then incubated with E-cadherin (1:25) or Vimentin antibody (1:50), followed by Alexa Fluor 568 (red)-conjugated goat anti-rabbit secondary antibody (ThermoFisher Scientific) or Alexa Fluor 488 (green)-conjugated goat anti-rabbit secondary antibody (ThermoFisher Scientific) for 1 h at room temperature in the dark. Specimens were counterstained and mounted using VECTASHIELD Mounting Medium with DAPI (Vector Laboratories, Gdynia, Poland). Immunofluorescence was analyzed with a LSM 780 confocal microscopy (Zeiss, Jena, Germany).

Human mRNA microarray analysis

Microarray analysis was performed using SurePrint G3 Human GE 8 × 60 K Microarray Ver3.0 (Agilent Technologies, Santa Clara, CA) and Feature Extraction Software (Agilent Technologies), according to the manufacture's protocol. Differentially expressed genes (DEGs) were selected

according to the manufacture's instruction, that is, they were selected based on a $\log_2$ fold change greater than 1 or lesser than -1. Gene ontology and pathway analyses were performed using DAVID v6.8 (https://david.ncifcrf.gov), while pathway analyses were performed using the database of Kyoto Encyclopedia of Genes and Genomes (KEGG, https://www.genome.jp/kegg/). Processes and pathways were regarded as significant at a *p value* less than 0.01.

Western blotting

Western blotting was performed as previously described [15]: in short, whole-cell lysates were prepared, and equivalent amounts of protein extracts were resolved using 12% SDS/PAGE, and were then transferred to polyvinylidene difluoride (PVDF) membranes (Merck, Darmstadt, Germany), which were blocked with BlockAce (KAC) and further incubated with primary antibodies against MAP1LC3B (1:1,000), p62 (1:2,000), and actin (C-11) (1:1,000) at 4 °C overnight. After the incubation with primary antibodies, the secondary antibody horseradish peroxidase-conjugated anti-rabbit or anti-goat immunoglobulin G (1:2,000) (Dako) was added, and the membranes were incubated at room temperature for 30 min. The immunoreactive bands were visualized with ImageQuant LAS4000 (GE Healthcare) and the densities of LC3B, p62, and actin were measured using ImageJ software (https://imagej.nih.gov/ij/).

Statistical analysis

The statistical significance of differences between groups was analyzed using Student's *t* test or Mann–Whitney U test. At least three independent replicates were assessed in each experiment, and pooled data are presented as mean ± standard error. Statistical analyses were performed using Microsoft Excel 2016 (Microsoft Office 2016; Microsoft, Redmond, WA) and figures were constructed using GraphPad Prism 7.0 software (GraphPad, La Jolla, CA). A *p-value* less than 0.05 was considered statistically significant.

Results

ULK2 is silenced by DNA methylation in diffuse-type gastric cancers

We performed genome-wide DNA methylation analysis on six gastric cancer tissues and four *Helicobacter pylori (H.pylori)* -negative normal tissues using HumanMethylation450K to identify *Atg* genes that were methylated in gastric cancer and unmethylated in normal gastric epithelium. Among 34 previously reported *Atg* genes, we were able to identify *MAP1LC3A*, *ULK2* and *ATG2A* [14, 16]. Likewise, we reported the methylation silencing of *MAP1LC3A* promotes gastric carcinogenesis [14]. *ULK2* has been reported about the association with cancer, but *ATG2A* has not been reported. Thus, for the subsequent analysis, we focused on *ULK2*.

ULK2 mRNA expression was assessed in human gastric tissues, including 30 gastric cancer tissues and five *H.pylori*-negative normal tissues, which showed *ULK2* mRNA expression of gastric cancer tissues was significantly lower than *H.pylori*-negative normal tissues (Fig. 1a) while the *ULK2* methylation level of gastric cancer tissues was higher than *H. pylori*-negative normal tissues (Fig. 1b). In its turn, we confirmed *ULK2* methylation level of poorly differentiated gastric cancers was significantly higher than well differentiated gastric cancers and *ULK2* methylation negatively correlated to *ULK2* mRNA expression from the TCGA database (Fig. 1c and Supplementary Fig. 1*a*).

The ULK2 expression profile was examined in four normal gastric tissues and four intestinal-type gastric cancers (IGC) and six DGC by immunohistochemistry to investigate the association between the histological type of gastric cancer and the ULK2 expression. ULK2 was strongly expressed in normal gastric epithelial cells and IGC, as expected, but it was not detected in DGC (Fig. 1d), whereas ULK2 score index of normal gastric epithelial cells and IGC were significantly higher than DGC (Fig. 1e). Interestingly, ULK2 was not detected in three small DGC on an early stage (Supplementary Fig. 1*b*), while in four mixed-type gastric cancers, ULK2 was expressed in intestinal component but not expressed in diffuse components (Supplementary Fig. 1*c*). Moreover, the staining pattern proved to be consistent in all the tissues tested.

To confirm whether DNA methylation silences *ULK2* in DGC, the DNA methylation status of *ULK2* was examined in two DGC tissues, from which adequate DNA was successfully extracted. *ULK2* was methylated in the cancer components and unmethylated in the corresponding adjacent normal components in both tissues (Fig. 1f).

Additionally, we explored the prognostic significance of ULK2 in gastric cancer using the database Kaplan–Meier Plotter (http://kmplot.com). Median overall survival was not significantly different between low and high expression groups of *ULK2* mRNA in gastric cancer patients (Supplementary Fig. 1d).

Knock-down of ULK2 promoted cell migration and EMT in gastric cancer cells

The mRNA expression of *ULK2* was examined in three human gastric cancer cell lines (NUGC3, MKN45, and AGS) by RT-PCR. The expression was at a significant level in NUGC3 and MKN45 cells, and was absent in AGS

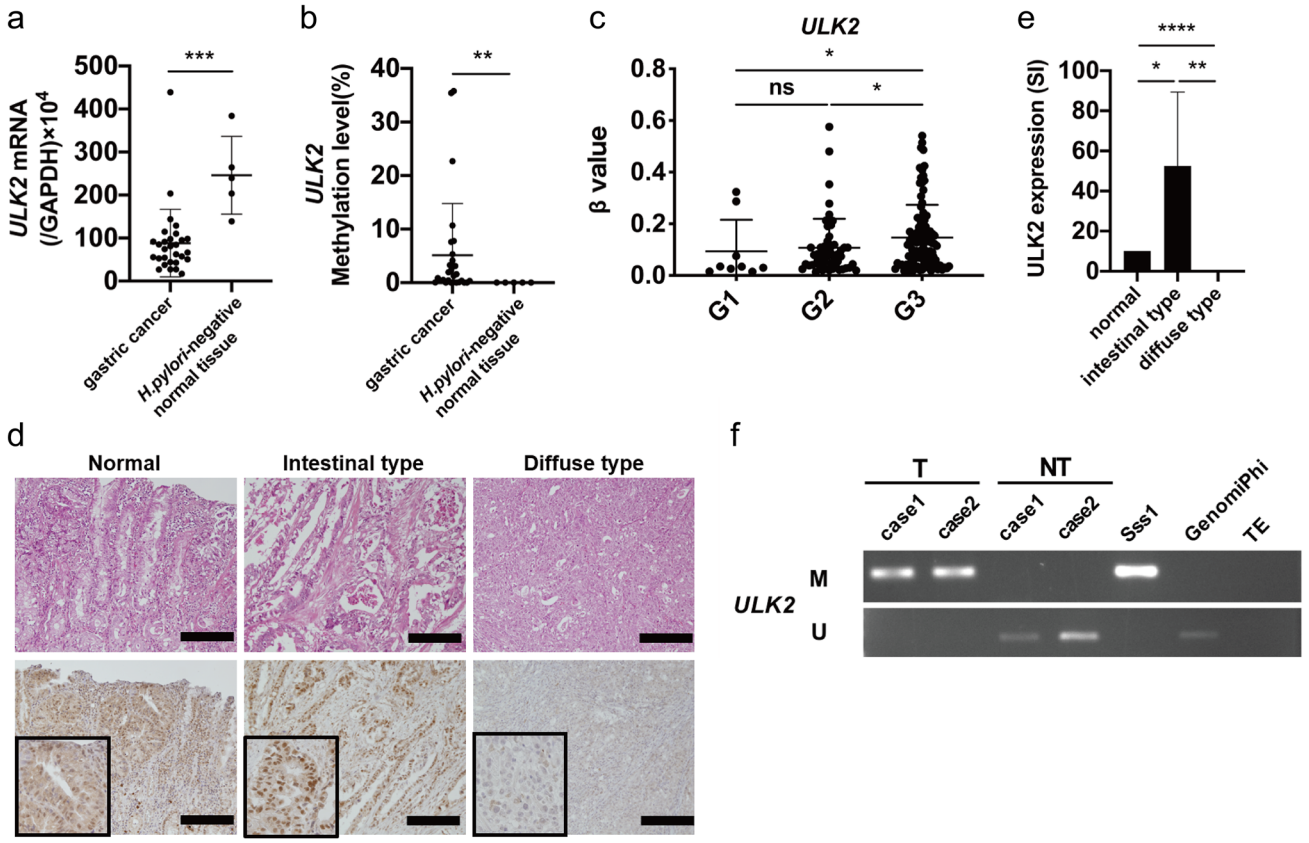

Fig. 1 *ULK2* is silenced by DNA methylation in diffuse-type gastric cancers. **a** RT-qPCR **b** qMSP in gastric cancer ($n=30$) and *H.pylori*-negative normal tissue ($n=5$) from biopsy samples. **c** β values of *ULK2* CpG island were taken from the TCGA database. G1, well-differentiated cancer ($n=9$); G2, moderately differentiated cancer ($n=51$); G3, poorly differentiated cancer ($n=100$). **d** Hematoxylin and eosin stain (upper) and immunohistochemical stain for ULK2 (lower) of human samples. The left panel indicates normal gastric epithelium, the median panel indicates intestinal-type gastric cancers and the right panel indicates diffuse-type gastric cancers. Representative images were shown. Black bar = 200 μ m. **e** ULK2 score index in normal gastric epithelium, intestinal-type and diffuse-type gastric cancers. **f** MSP of tumor and non-tumor tissues from FFPE specimens by microdissection methods in 2 cases of DGC. T, tumor; NT, non-tumor. The data represent the mean ± standard error of the mean in triplicate from one representative of three with similar results. NS, not significant; *, *p-value* < 0.05, **, *p-value* < *0.01*, ***, *p-value* < 0.001, ****, *p-value* < 0.0001, Student's *t* test in (**a**) (**b**) and (**e**), Mann–Whitney U test in (**c**)

cells (Fig. 2a). NUGC3 and MKN45 cells were, thus, used to investigate the function of ULK2.

In addition, *ULK2* was fully methylated without mRNA expression in AGS cells (Fig. 2a and 2b), whereas the demethylation treatment significantly decreased the methylation level while increasing *ULK2* mRNA expression in AGS cells (Fig. 2c). These results indicate *ULK2* is regulated by DNA methylation in gastric cancer cell lines.

Knock-down of *ULK2* was successfully performed and the mRNA levels were decreased to 10–20% and 25–40% of the level in the control in NUGC3 and MKN45 cells, respectively (Fig. 2d). Migration assay was performed with *ULK2* knock-downed cells to assess the effect of ULK2 on cell migration, which then showed the migration of *ULK2* knock-downed cells was more promoted than that of control cells in both NUGC3 and MKN45 cells (Fig. 2e).

Additionally, we evaluated the expressions of epithelial and mesenchymal markers in NUGC3 and MKN45 cells to examine the involvement of ULK2 in EMT. Knock-down of *ULK2* reduced the expression of E-cadherin, an epithelial marker protein, and enhanced the expression of Vimentin, a mesenchymal marker protein, in both NUGC3 and MKN45 cells (Fig. 2f). These results suggest that knock-down of *ULK2* can induce cell migration and EMT in gastric cancer cells.

Knock-down of ULK2-induced oncogenic pathways related to cell migration and EMT

To investigate the gene expression changes in NUGC3 and MKN45 cells by knock-down of *ULK2,* mRNA microarray analyses were performed, which identified 2,896 and 1,949

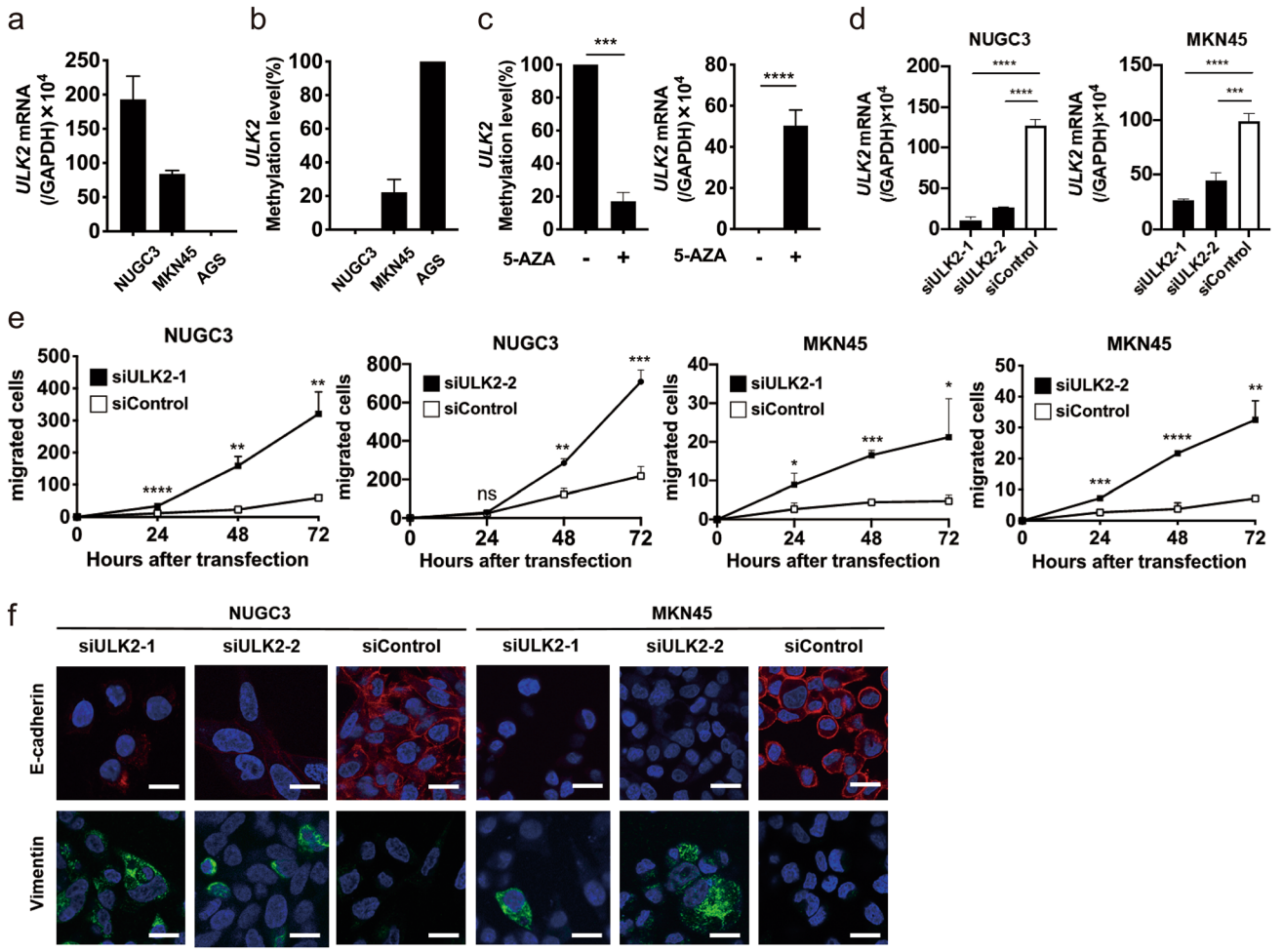

Fig. 2 Knock-down of *ULK2* induces cell migration and EMT in gastric cancer cells. **a** RT-qPCR **b** qMSP in NUGC3, MKN45 and AGS cells. **c** RT-qPCR and qMSP in AGS cell treated with de-methylation treatment. **d** RT-qPCR **e** Migration assay **f** Immunocytochemistry in NUGC3 and MKN45 treated with *siULK2* or *siControl*. The data represent the mean ± standard error of the mean in triplicate from one representative of three with similar results. *siULK2*, siRNA of *ULK2*; *siControl*, negative control siRNA; NS, not significant; *, *p-value* < 0.05, **, *p-value* < 0.01, ***, *p-value* < 0.001, ****, *p-value* < 0.0001, Student's *t* test

genes as DEGs in NUGC3 and MKN45 cells, respectively. 1,545 and 794 genes among the DEGs were upregulated by knock-down of *ULK2* in NUGC3 and MKN45 cells, respectively, and 92 genes were commonly upregulated, of which 23 were importantly associated with cell migration (red point) and 10 of these 23 genes were further associated with EMT (red name genes) (Fig. 3a and Supplementary Table 3). 1,351 and 1,152 genes were, on the other hand, downregulated in NUGC3 and MKN45 cells, respectively, and 225 genes were commonly downregulated. Also, 15 of these 225 genes were importantly associated with cell migration (red point), with 4 of these 15 being associated with EMT (red name genes) (Fig. 3b and Supplementary Table 4). Twenty-one and 19 of 38 genes associated with cell migration were validated by RT-PCR in NUGC3 and MKN45 cells, respectively, while 10 and 12 of 14 genes associated with EMT were validated by RT-PCR in NUGC3 and MKN45 cells, respectively (Supplementary Fig. 2 and Supplementary Fig. 3).

The gene ontology analysis of DEGs showed that 60 and 43 biological processes were significantly enriched in *ULK2* knock-downed NUGC3 and MKN45 cells, respectively (Supplementary Table 5 and Supplementary Table 6), and that four among the top ten significant processes were likewise associated with cell adhesion and chemotaxis (Fig. 3c). The pathway analysis showed that 21 and 13 pathways were significantly enriched in *ULK2* knock-downed NUGC3 and MKN45 cells, respectively, and that chemokine signal pathway, cell adhesion molecules and focal adhesion were associated with cell migration or EMT (Fig. 3d). In other words, these results suggest that knock-down of *ULK2* can promote cell migration and EMT through expression changes in the corresponding genes.

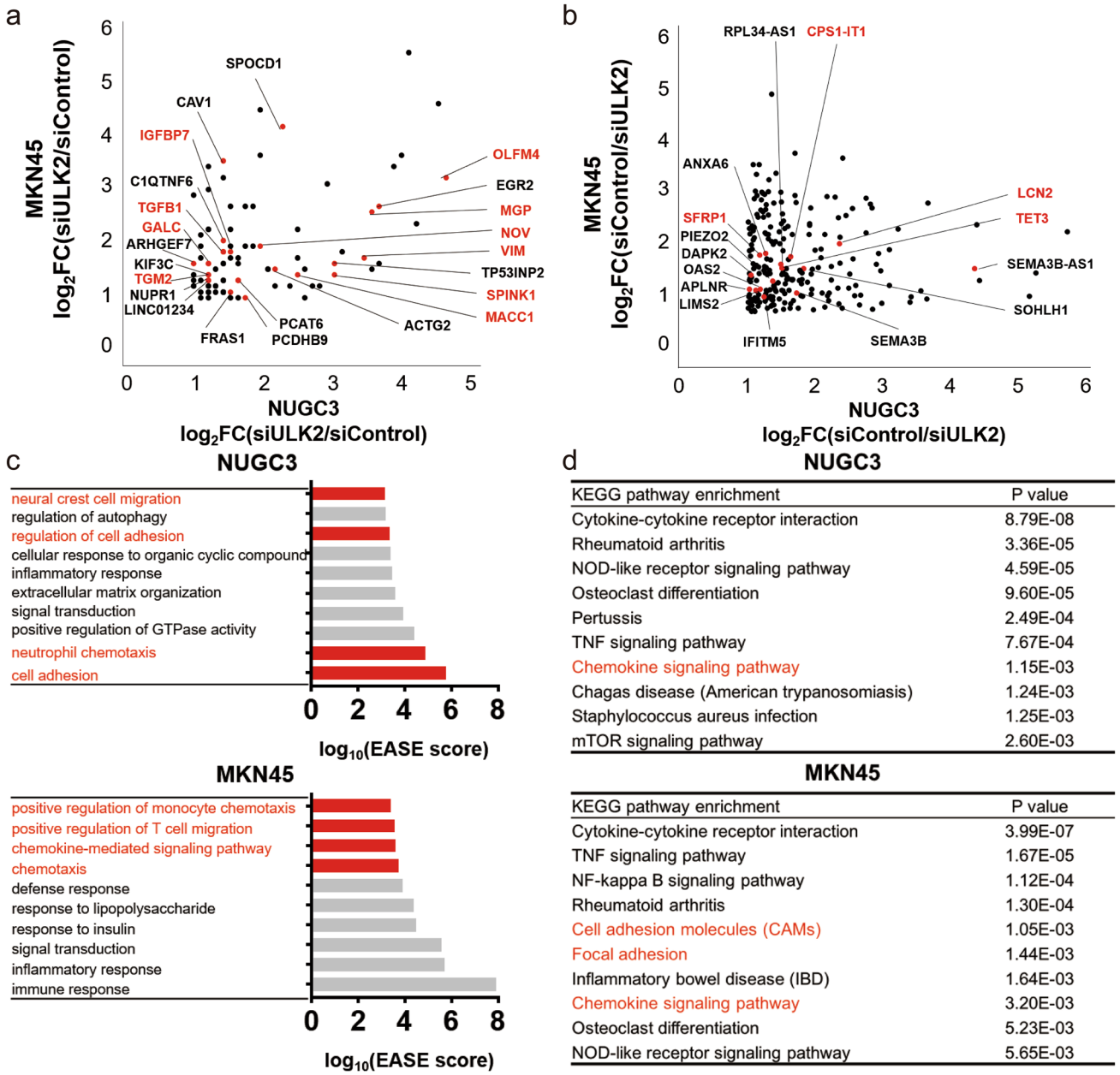

d

NUGC3

KEGG pathway enrichment	P value
Cytokine-cytokine receptor interaction	8.79E-08
Rheumatoid arthritis	3.36E-05
NOD-like receptor signaling pathway	4.59E-05
Osteoclast differentiation	9.60E-05
Pertussis	2.49E-04
TNF signaling pathway	7.67E-04
Chemokine signaling pathway	1.15E-03
Chagas disease (American trypanosomiasis)	1.24E-03
Staphylococcus aureus infection	1.25E-03
mTOR signaling pathway	2.60E-03

MKN45

KEGG pathway enrichment	P value
Cytokine-cytokine receptor interaction	3.99E-07
TNF signaling pathway	1.67E-05
NF-kappa B signaling pathway	1.12E-04
Rheumatoid arthritis	1.30E-04
Cell adhesion molecules (CAMs)	1.05E-03
Focal adhesion	1.44E-03
Inflammatory bowel disease (IBD)	1.64E-03
Chemokine signaling pathway	3.20E-03
Osteoclast differentiation	5.23E-03
NOD-like receptor signaling pathway	5.65E-03

Fig. 3 Knock-down of *ULK2* induces the oncogenic pathway in gastric cancer cells. Microarray analysis in NUGC3 treated with *siULK2-1* or *siControl* and MKN45 treated with *siULK2-2* or *siControl*. **a** Upregulated genes by *siULK2* were shown in black point ($\log_2$ fold change≧1). Cell migration related genes were shown in red point. EMT-related genes were shown in red name. **b** Downregulated genes by *siULK2* were shown in black point ($\log_2$ fold change≧1). Cell migration related genes were shown in red point. EMT-related genes were shown in red name. **c** The top ten processes from the gene ontology analysis ranked by *p-value*, shown as a bar chart. Red bar indicates cell adhesion, migration and chemotaxis related processes. **d** The top ten pathways from the KEGG pathway enrichment analysis ranked by *p value*. The pathway related to cell migration and adhesion were shown in red name. *siULK2*, siRNA of *ULK2*; *siControl*, negative control siRNA; $\log_2$FC (*siULK2*/*siControl*), $\log_2$ fold change between the gene expression of *siULK2* cells and *siControl* cells; $\log_{10}$ (EASE score), -$\log_{10}$ *p- value*

Knock-down of ULK2 promoted cell migration and EMT via autophagy induction

Without any autophagy inducer, knock-down of *ULK2* reduced p62, which is degraded by autophagy processes and used as an autophagy marker, in NUGC3 cells and enhanced the conversion of cytosolic LC3B (LC3B-I) to auto-phagosomal membrane-associated LC3B (LC3B-II) in both cells (Fig. 4a and Supplementary Fig. 4*a*), which indicate that knock-down of *ULK2* can induce autophagy independently.

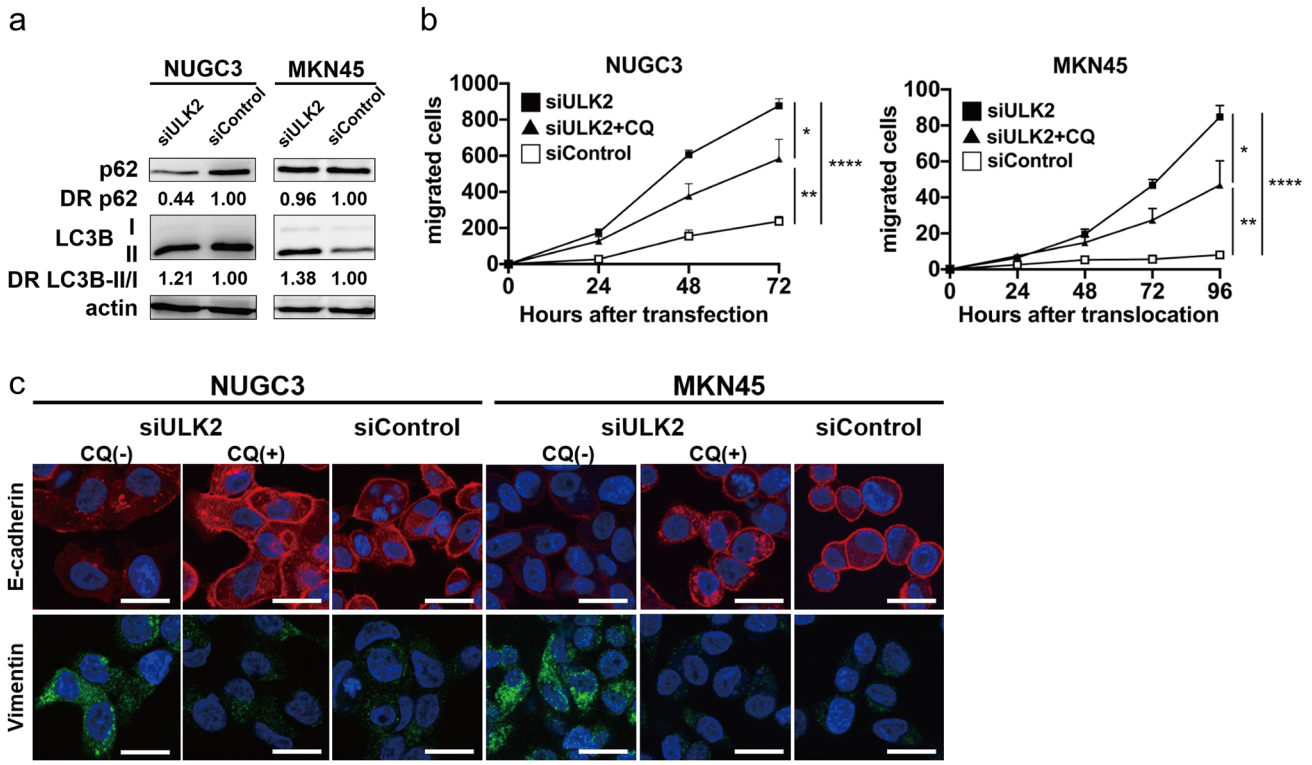

Fig. 4 Knock-down of *ULK2* enhances autophagy and induces cell migration and EMT dependent on autophagy induction, **a** Western blotting in NUGC3 treated with *siULK2-1* or *siControl* and MKN45 treated with *siULK2-2 or siControl*. β-actin was used as an internal control. Densities of each bands were measured using ImageJ and the ratio were calculated. LC3B-II/I was defined as density value of LC3B-II/density value of LC3B-I. **b** Migration assay **c** Immunocytochemistry in NUGC3 treated with *siULK2-1* or *siControl* and MKN45 treated with *siULK2-2 or siControl*. Addition of CQ inhibited the effects of *siULK2*. *siULK2*, siRNA of *ULK2*; *siControl*, negative control siRNA; DR, density ratio; *, *p-value* < 0.05, **, *p-value* < 0.01, ****, *p-value* < 0.0001, Student's *t* test

We used CQ, an autophagy lysosomal inhibitor, to investigate the role of autophagy in ULK2-induced cell migration and EMT. CQ inhibited autophagy induction in *ULK2* knock-downed NUGC3 (Supplementary Fig. 4*b)*, and cell migration in both NUGC3 and MKN45 (Fig. 4b and Supplementary Fig. 4*c*). Furthermore, CQ enhanced the expression of E-cadherin and reduced the expression of Vimentin in both *ULK2* knock-downed NUGC3 and MKN45 cells (Fig. 4c and Supplementary Fig. 4*d*). These results suggest that knock-down of *ULK2* can promote cell migration and EMT dependent on autophagy induction.

Discussion

In this study, we have demonstrated that *ULK2* was specifically silenced by DNA methylation in DGC. Additionally, knock-down of *ULK2* enhanced autophagy and induced cell migration and EMT through expression changes in the corresponding genes in gastric cancer cells. Our findings indicate that down-regulation of *ULK2* can cause transformation to DGC.

Autophagy plays an important role in the migration and EMT of various cancer cells [6]. The induction of autophagy by hypoxic inducible factor (HIF)-1α can promote EMT in pancreatic cancer stem cells [17]. Furthermore, sphingosine kinase 1 (SPHK1) can promote cell migration in hepatocellular carcinoma cells through the activation of TNF receptor-associated factor 2 (TRAF2)-mediated autophagy [18]. Death effector domain-containing DNA-binding protein (DEDD)-induced autophagy can, in contrast, inhibit EMT in breast cancers through the degradation of Snail and Twist [19]. These findings suggest that autophagy might have cancer type-dependent functions in cell migration and EMT.

The ULK1/2 complex plays an essential role in the initiation of autophagy, having various functions, such as cell fate determination, metabolism, transcriptional control and neurite development [10]. ULK1 and ULK2 share a 78% homology within their protein kinase domains. ULK2 is expressed ubiquitously, and, at first glance, its function appears to be redundant with that of ULK1, which is predominantly located in the cytosol whereas ULK2 is predominantly located in the nucleus [11]. Recent studies showed that ULK1 was over-expressed in gastric cancer [20], whereas

miR-1262 and *circular RNA TMEM87A* upregulated ULK1 expression and induced cell proliferation and migration [21, 22]. In this study, we showed that ULK2 was downregulated in gastric cancer and that this induced cell migration and EMT. Thus, although the detailed relationship between ULK1 and ULK2 has yet to be clarified, ULK1 and ULK2 might play opposite roles in gastric cancer.

Recent studies reported knock-down of *ULK2* induced autophagy and promoted EMT in A549, a lung cancer cell line [12]. Before our study, however, it was unclear how knock-down of *ULK2* induced EMT. In the current study, we showed that CQ inhibited cell migration and EMT induced by knock-down of *ULK2* in gastric cancer cell lines. Furthermore, we were able to confirm knock-down of *ULK2* changed the expressions of oncogenic 38 genes that are associated with cell migration and EMT, including *OLFM4, EGR2, MGP*, *VIM*, *TP53INP2, SPINK1*, *MACC1*, *SPOCD1*, *ACTG2*, *NOV*, *PCDHB9*, *PCAT6*, *FRAS1, C1QTNF6, CAV1, KIF3C, GALC, LINC01234, ARHGEF7, IGFBP7, TGFBI, NUPR1, TGM2, SEMA3B-AS1, SEMA3B, SOHLH1, CPS1-IT1, RPL34-AS1, PIEZO2, IFITM5, ANXA6, OAS2, LIMS2, DAPK2, TET3, SFRP1, LCN2 and APLNR* [23–59]. We validated 21 and 19 genes of them in NUGC3 and MKN45 cells, respectively, by RT-PCR. Therefore, we showed that knock-down of *ULK2* promotes cell migration and EMT through autophagy induction.

In spite of its clinical significance being unclear, *ULK2* was reported to be downregulated in glioblastoma and lung cancer [12, 60]. In this regard, we found that ULK2 was strongly expressed in IGC, but was scarcely expressed in DGC, which can be divided into two groups according to the tumor development process. Originally, one group includes diffuse-type cancers only, without a component of intestinal-type cancers, while the other includes diffuse-type cancers derived from intestinal-type cancers, which sometimes have two components of diffuse-type and intestinal-type cancers in the same cancer tissue (mixed type). In three small DGC on an early stage, limited ULK2 expression was detected in the cancer tissue, which suggested *ULK2* had already been downregulated in the early stage of carcinogenesis of DGC and that the down-regulation of *ULK2* might directly cause DGC from pre-malignant tissues. In four mixed-type gastric cancers, ULK2 was definitely detected in the intestinal component but it was not detected in the diffuse component in all the four tissues, which in turn suggests that the down-regulation of *ULK2* can transform intestinal-type cancer cells into diffuse-type cancer cells. Bearing in mind these results, the down-regulation of *ULK2* could be associated with the development of DGC directly from pre-malignant tissues and IGC. Lauren classification is an independent predictor for overall survival in gastric cancer and IGC presents better survival than DGC [4]. Although our study suggested that *ULK2* silencing could cause DGC characteristics, *ULK2* expression was not associated with overall survival in gastric cancer patients of Kaplan–Meier Plotter database. The unexpected results might be brought because the analysis was performed retrospectively. A prospective study would resolve this matter.

ULK2 gene mutations, including synonymous and non-synonymous mutations, were detected in 1 of 81 (1.23%) cases of DGC and 5 of 174 (2.87%) cases of IGC, according to the TCGA database. These results suggest that gene mutations have a limited contribution to the down-regulation of *ULK2* in gastric cancers. microRNA.org (www.microrna.org) additionally showed that 75 miRNAs could target *ULK2*, and that among these miRNAs the down-regulation of *miRNA-26b* inhibited cell proliferation by targeting *ULK2* and inactivating the *PTEN/AKT* pathway in laryngeal cancer cells [61]. In this study, we found that *ULK2* was silenced by DNA methylation in clinical samples of DGC and a gastric cancer cell line. DNA methylation, therefore, mainly contributes to the down-regulation of *ULK2* in gastric cancers.

This study has some limitations. First, we could not clarify the mechanisms through which the down-regulation of *ULK2* induced cell migration and EMT. However, we were able to show for the first time that down-regulation of *ULK2* enhanced the gene expression associated with cell migration and EMT. Second, the sample size was small for immunohistochemistry, but the expression pattern, which proved to be weak in normal gastric epithelial cells, strong in intestinal-type gastric cancer cells and limited in diffuse-type gastric cancer cells, was consistent in all the investigated samples.

In conclusion, this is the first study to confirm that *ULK2* was specifically silenced by DNA methylation in DGC, demonstrating that knock-down of *ULK2* promotes cell migration and EMT through the induction of autophagy in gastric cancer cells. The methylation silencing of *ULK2,* therefore, causes the transformation to poorly differentiated cancers through the induction of EMT.

Supplementary Information The online version contains supplementary material available at https://doi.org/10.1007/s10120-021-01250-0.

Acknowledgements The authors thank Ms. Toyomi Kozawa (University of Toyama) for providing technical support in all of these experiments. This work was supported by JSPS KAKENHI Grants (JP15K19317 and JP18K15806).

Declarations

Conflict of interest The authors hold no conflicts.

References

1. Van Cutsem E, Sagaert X, Topal B, Haustermans K, Prenen H. Gastric cancer. Lancet. 2016;388:2654–64.

2. Lauren P. The two histological main types of gastric carcinoma: diffuse and so-called intestinal-type carcinoma. An attempt at a histo-clinical classification. Acta Pathol Microbiol Scand. 1965;64(1):31–49.
3. Chiaravalli AM, Klersy C, Vanoli A, Ferretti A, Capella C, Solcia E. Histotype-based prognostic classification of gastric cancer. World J Gastroenterol. 2012;18:896–904.
4. Chen YC, Fang WL, Wang RF, Liu CA, Yang MH, Lo SS, et al. Clinicopathological variation of Lauren classification in gastric cancer. Pathol Oncol Res. 2016;22:197–202.
5. Ge S, Xia X, Ding C, Zhen B, Zhou Q, Feng J, et al. A proteomic landscape of diffuse-type gastric cancer. Nat Commun. 2018;9(1):1012.
6. Colella B, Faienza F, Di Bartolomeo S. EMT regulation by autophagy: a new perspective in glioblastoma biology. Cancers. 2019;11:312–32.
7. Choi AMK, Ryter SW, Levine B. Autophagy in human health and disease. N Engl J Med. 2013;368:651–62.
8. White E. Deconvoluting the context-dependent role for autophagy in cancer. Nat Rev Cancer. 2012;12:401–10.
9. Levine B, Kroemer G. Autophagy in the pathogenesis of disease. Cell. 2008;132:27–42.
10. Shin SH, Lee EJ, Chun J, Hyun S, Kang SS. ULK2 Ser 1027 Phosphorylation by PKA Regulates Its Nuclear Localization Occurring through Karyopherin Beta 2 Recognition of a PY-NLS Motif. PLOS ONE. 2015;10:e0127784.
11. Lee EJ, Tournier C. The requirement of uncoordinated 51-like kinase 1 (ULK1) and ULK2 in the regulation of autophagy. Autophagy. 2011;7:689–95.
12. Kim YH, Baek SH, Kim EK, Ha JM, Jin SY, Lee HS, et al. Uncoordinated 51-like kinase 2 signaling pathway regulates epithelial-mesenchymal transition in A549 lung cancer cells. FEBS Lett. 2016;590:1365–74.
13. Shukla S, Patric IR, Patil V, Shwetha SD, Hegde AS, Chandramouli BA, et al. Methylation silencing of ULK2, an autophagy gene, is essential for astrocyte transformation and tumor growth. J Biol Chem. 2014;289:22306–18.
14. Muhammad JS, Nanjo S, Ando T, Yamashita S, Maekita T, Ushijima T, et al. Autophagy impairment by Helicobacter pylori-induced methylation silencing of MAP1LC3Av1 promotes gastric carcinogenesis. Int J Cancer. 2017;140:2272–83.
15. Ando T, Yoshida T, Enomoto S, Asada K, Tatematsu M, Ichinose M, et al. DNA methylation of microRNA genes in gastric mucosae of gastric cancer patients: its possible involvement in the formation of epigenetic field defect. Int J Cancer. 2009;124:2367–74.
16. Pyo JO, Nah J, Jung YK. Molecules and their functions in autophagy. Exp Mol Med. 2012;44:73–80.
17. Zhu H, Wang D, Zhang L, Xie X, Wu Y, Liu Y, et al. Upregulation of autophagy by hypoxia-inducible factor-1alpha promotes EMT and metastatic ability of CD133+ pancreatic cancer stem-like cells during intermittent hypoxia. Oncol Rep. 2014;32:935–42.
18. Liu H, Ma Y, He HW, Zhao WL, Shao RG. SPHK1 (sphingosine kinase 1) induces epithelial-mesenchymal transition by promoting the autophagy-linked lysosomal degradation of CDH1/E-cadherin in hepatoma cells. Autophagy. 2017;13:900–13.
19. Lv Q, Hua F, Hu ZW. DEDD, a novel tumor repressor, reverses epithelial-mesenchymal transition by activating selective autophagy. Autophagy. 2012;8:1675–6.
20. Chen MB, Ji XZ, Liu YY, Zeng P, Xu XY, Ma R, et al. Ulk1 overexpression in human gastric cancer is correlated with patients' T classification and cancer relapse. Oncotarget. 2017;8:33704–12.
21. Zheng Y, Xie M, Zhang N, Liu J, Song Y, Zhou L, Yang M. miR-1262 suppresses gastric cardia adenocarcinoma via targeting oncogene *ULK1*. J Cancer. 2021;12:1231–9.
22. Wang H, Sun G, Xu P, Lv J, Zhang X, Zhang L, et al. Circular RNA TMEM87A promotes cell proliferation and metastasis of gastric cancer by elevating ULK1 via sponging miR-142-5p. J Gastroenterol. 2021;56:125–38.
23. Xiong B, Lei X, Zhang L, Fu J. miR-103 regulates triple negative breast cancer cells migration and invasion through targeting olfactomedin 4. Biomed Pharmacother. 2017;89:1401–8.
24. Li X, Zhang Z, Yu M, Li L, Du G, Xiao W, Yang H, et al. Involvement of miR-20a in promoting gastric cancer progression by targeting early growth response 2 (EGR2). Int J Mol Sci. 2013;14(8):16226–39.
25. Mertsch S, Schurgers LJ, Weber K, Paulus W, Senner V. (2009) Matrix gla protein (MGP): an overexpressed and migration-promoting mesenchymal component in glioblastoma. BMC Cancer; 9(1):302–12302–12.
26. Lu R, Zhou ZQ, Yu WF, Xia YF, Zhi XT. CPEB4 promotes cell migration and invasion via upregulating vimentin expression in breast cancer. Biochem Biophys Res Commun. 2017;489:135–41.
27. Moran-Jones K, Grindlay J, Jones M, Smith R, Norman JC. hnRNP A2 regulates alternative mRNA splicing of TP53INP2 to control invasive cell migration. Cancer Res. 2009;69:9219–27.
28. Xu L, Lu C, Huang Y, Zhou J, Wang X, Liu C, et al. SPINK1 promotes cell growth and metastasis of lung adenocarcinoma and acts as a novel prognostic biomarker. BMB Rep. 2018;51:648–53.
29. Li Z, Guo T, Fang L, Li N, Wang X, Wang P, et al. MACC1 overexpression in carcinoma-associated fibroblasts induces the invasion of lung adenocarcinoma cells via paracrine signaling. Int J Oncol. 2019;54:1367–75.
30. Liu Q, Wang XY, Qin YY, Yan XL, Chen HM, Huang QD, et al. SPOCD1 promotes the proliferation and metastasis of glioma cells by up-regulating PTX3. Am J Cancer Res. 2018;8:624–35.
31. Wu Y, Liu ZG, Shi MQ, Yu HZ, Jiang XY, Yang AH, et al. Identification of ACTG2 functions as a promoter gene in hepatocellular carcinoma cells migration and tumor metastasis. Biochem Biophys Res Commun. 2017;491:537–44.
32. Liu S, Han L, Wang X, Liu Z, Ding S, Lu J, et al. Nephroblastoma overexpressed gene (NOV) enhances RCC cell motility through upregulation of ICAM-1 and COX-2 expression via Akt pathway. Int J Clin Exp Pathol. 2015;8:1302–11.
33. Mukai S, Oue N, Oshima T, Imai T, Sekino Y, Honma R, et al. Overexpression of PCDHB9 promotes peritoneal metastasis and correlates with poor prognosis in patients with gastric cancer. J Pathol. 2017;243:100–10.
34. Cui LH, Xu HR, Yang W, Yu LJ. lncRNA PCAT6 promotes non-small cell lung cancer cell proliferation, migration and invasion through regulating miR-330-5p. Onco Targets Ther. 2018;11:7715–24.
35. Zhan Q, Huang RF, Liang XH, Ge MX, Jiang JW, Lin H, Zhou XL. FRAS1 knockdown reduces A549 cells migration and invasion through downregulation of FAK signaling. Int J Clin Exp Med. 2014;7:1692–7.
36. Qu HX, Cui L, Meng XY, Wang ZJ, Cui YX, Yu YP, et al. C1QTNF6 is overexpressed in gastric carcinoma and contributes to the proliferation and migration of gastric carcinoma cells. Int J Mol Med. 2019;43:621–9.
37. Wang Y, Song Y, Che X, Zhang L, Wang Q, Zhang X, et al. Caveolin-1 enhances RANKL-induced gastric cancer cell migration. Oncol Rep. 2018;40:1287–96.
38. Wang C, Wang C, Wei Z, Li Y, Wang W, Li X, et al. Suppression of motor protein KIF3C expression inhibits tumor growth and metastasis in breast cancer by inhibiting TGF-beta signaling. Cancer Lett. 2015;368:105–14.
39. Liu DG, Xue L, Li J, Yang Q, Peng JZ. Epithelial-mesenchymal transition and GALC expression of circulating tumor cells indicate metastasis and poor prognosis in non-small cell lung cancer. Cancer Biomark. 2018;22:417–26.
40. Ghaffar M, Khodahemmati S, Li JT, Shahzad M, Wang M, Wang YJQ, et al. Long non-coding RNA LINC01234 regulates

proliferation, invasion and apoptosis in esophageal cancer cells. J Cancer. 2018;9:4242–9.
41. Lei X, Deng L, Liu DN, Liao SJ, Dai H, Li JX, et al. ARHGEF7 promotes metastasis of colorectal adenocarcinoma by regulating the motility of cancer cells. Int J Oncol. 2018;53:1980–96.
42. Yue C, Yang M, Tian Q, Mo F, Peng J, Ma Y, et al. IGFBP7 is associated to prognosis and could suppress cell survival in cholangiocarcinoma. Artif Cells Nanomed Biotechnol. 2018;46:817–25.
43. Guo SK, Shen MF, Yao HW, Liu YS. Enhanced expression of TGFBI promotes the proliferation and migration of glioma cells. Cell Physiol Biochem. 2018;49:1097–109.
44. Emma MR, Iovanna JL, Bachvarov D, Puleio R, Loria GR, Augello G, et al. NUPR1, a new target in liver cancer: implication in controlling cell growth, migration, invasion and sorafenib resistance. Cell Death Dis. 2016;7:e2269.
45. Fuja DG, Rainusso NC, Shuck RL, Kurenbekova L, Donehower LA, Yustein JT. Transglutaminase-2 promotes metastatic and stem-like phenotypes in osteosarcoma. Am J Cancer Res. 2018;8:1752–63.
46. Guo W, Liang X, Liu L, Guo Y, Shen S, Liang J, Dong Z, et al. MiR-6872 host gene SEMA3B and its antisense lncRNA SEMA3B-AS1 function synergistically to suppress gastric cardia adenocarcinoma progression. Gastric Cancer. 2019;22(4):705–22.
47. Liu X, Gao Q, Zhao N, Zhang X, Cui W, Sun J, et al. Sohlh1 suppresses glioblastoma cell proliferation, migration, and invasion by inhibition of Wnt/beta-catenin signaling. Mol Carcinog. 2018;57:494–502.
48. Zhang W, Yuan W, Song J, Wang S, Gu X. LncRna CPS1-IT1 suppresses cell proliferation, invasion and metastasis in colorectal cancer. Cell Physiol Biochem. 2017;44:567–80.
49. Gong Z, Li J, Cang P, Jiang H, Liang J, Hou Y. RPL34-AS1 functions as tumor suppressive lncRNA in esophageal cancer. Biomed Pharmacother 2019;120:109440.
50. Huang Z, Sun Z, Zhang X, Niu K, Wang Y, Zheng J, et al. Loss of stretch-activated channels, PIEZOs, accelerates non-small cell lung cancer progression and cell migration. Biosci Rep 2019;39:BSR20181679.
51. Liu BY, Lu YQ, Han F, Wang Y, Mo XK, Han JX. Effects of the overexpression of IFITM5 and IFITM5 c.-14C>T mutation on human osteosarcoma cells. Oncol Lett 2017;13:111–8.
52. García-Melero A, Reverter M, Hoque M, Meneses-Salas E, Koese M, Conway JR, et al. Annexin A6 and late endosomal cholesterol modulate integrin recycling and cell migration. J Biol Chem. 2016;291:1320–35.
53. Kim JC, Ha YJ, Tak KH, Roh SA, Kwon YH, Kim CW, et al. Opposite functions of GSN and OAS2 on colorectal cancer metastasis, mediating perineural and lymphovascular invasion, respectively. PLOS ONE. 2018;13:e0202856.
54. Kim SK, Jang HR, Kim JH, Noh SM, Song KS, Kim MR, et al. The epigenetic silencing of LIMS2 in gastric cancer and its inhibitory effect on cell migration. Biochem Biophys Res Commun. 2006;349:1032–40.
55. Ivanovska J, Zlobec I, Forster S, Karamitopoulou E, Dawson H, Koelzer VH, et al. DAPK loss in colon cancer tumor buds: implications for migration capacity of disseminating tumor cells. Oncotarget. 2015;6:36774–88.
56. Ye Z, Li J, Han X, Hou H, Chen H, Zheng X, et al. TET3 inhibits TGF-β1-induced epithelial-mesenchymal transition by demethylating miR-30d precursor gene in ovarian cancer cells. J Exp Clin Cancer Res. 2016;35:72–8172.
57. Ren J, Wang R, Huang G, Song H, Chen Y, Chen L. sFRP1 inhibits epithelial-mesenchymal transition in A549 human lung adenocarcinoma cell line. Cancer Biother Radiopharm. 2013;28:565–71.
58. Feng M, Feng J, Chen W, Wang W, Wu X, Zhang J, et al. Lipocalin2 suppresses metastasis of colorectal cancer by attenuating NF-κB-dependent activation of snail and epithelial mesenchymal transition. Mol Cancer. 2016;15:77.
59. Roche J, Ramé C, Reverchon M, Mellouk N, Cornuau M, Guerif F, et al. Apelin (APLN) and apelin receptor (APLNR) in human ovary: expression, signaling, and regulation of steroidogenesis in primary human luteinized granulosa cells. Biol Reprod. 2016;95:104.
60. Cheng H, Yang ZT, Bai YQ, Cai YF, Zhao JP. Overexpression of Ulk2 inhibits proliferation and enhances chemosensitivity to cisplatin in non-small cell lung cancer. Oncol Lett. 2019;17:79–86.
61. Wang S, Guo D, Li C. Downregulation of miRNA-26b inhibits cancer proliferation of laryngeal carcinoma through autophagy by targeting ULK2 and inactivation of the PTEN/AKT pathway. Oncol Rep. 2017;38:1679–87.